

Turbulence statistics in solid-liquid flow using a refractive index matching and particle image velocimetry technique

Yogesh K.Agrawal¹, Roohi Shokri², R. Sean Sanders², David S. Nobes¹

¹Department of Mechanical Engineering, University of Alberta, Edmonton, Canada

²Department of Chemical and Material Engineering, University of Alberta, Edmonton, Canada

*corresponding author: dnobes@ualberta.ca

Abstract: Turbulence statistics of solid-liquid slurry flow are measured using particle image velocimetry (PIV). Experiments are carried out in a 50.6 mm inner diameter vertical pipe loop for Reynolds number (Re) 320,000 with 0.8% particle volume concentration. Water and nearly monosized 2 mm glass beads are used as carrier and dispersed phases, respectively. During PIV post processing, particle masking is used to identify slurry particles and allow calculation of instantaneous velocity of both phases. Liquid phase axial and radial turbulent fluctuation velocity profiles are obtained from instantaneous velocity data of just the single-phase and compared with both solids and fluid in two-phase flow. The presence of the dispersed phase has no significant effect on liquid phase turbulence for 0.8% particle concentration. PIV, in conjunction with phase separation in collected images is only practicable for particle concentrations less than 1%. At higher concentrations, phase boundaries produce an unacceptable level of light scattering. To test more concentrated slurries, a refractive index matching technique, in combination with PIV, is utilized. In this experimental study, an alternative index matching fluid (aqueous potassium thiocyanate solution) is compared with a sodium iodide solution, which has been more commonly used for refractive index matching studies. The present study describes the use of a 62.4% (by mass) solution of KSCN in water, along with monosized 3 mm borosilicate glass beads for measurements of concentrated slurry flows.

Keywords: turbulence, refractive index matching, PIV, slurry flow

1 Introduction

Two-phase flows are widely encountered in engineering and natural processes. In particular, solid-liquid flows (also known as slurry flows) have important applications in numerous industrial and chemical processes [1]. Transportation of coal, ore, and oil sands in slurry flows by pipelines are often turbulent in nature [2]. The presence of particles (dispersed phase) in solid-liquid flows has a major impact on turbulent heat and momentum transfer properties of the liquid (continuous) phase [3]. Experiments have shown, for specific two-phase systems, how the presence of the particles can affect the turbulence structure of the liquid [4]. Mechanisms through which the dispersed (particulate) phase affects fluid turbulence are poorly understood but researchers suggest that turbulence augmentation is governed by the creation of wakes behind the particles while attenuation may be related to through interference with and/or breakup of existing eddies [2][5]. However, no experiments have been conducted to investigate the turbulence statistics for high Reynolds number flows of concentrated slurries.

Experimental studies of solid-liquid flows are frequently conducted by optical and flow visualization techniques such as laser Doppler velocimetry (LDV), particle image velocimetry (PIV) and particle tracking velocimetry (PTV) [6]. Over the last two decades, PIV has become a promising tool for two-phase flows, due to its ability to provide simultaneous velocity measurements of both phases [2]. PIV measurements are significantly more difficult in two-phase flows compared with single-phase flows as the dispersed phase limits the length or penetration depth of the laser sheet into the flow and significant light scattering can occur [7]. However, application of PIV with special phase discrimination and processing techniques such as the use of fluorescent particles with a dual camera system, particle masking and correlation peak separation method has been used to eliminate phase boundaries in two-phase flow [8].

A slurry mixture is difficult to penetrate optically even at a dispersed phase concentration of 1% due to high opacity of the dispersed phase and high degree of light scattering, generating laser light flare [9]. This indicates

that conventional PIV systems, even in combination with image processing for phase separation, cannot be used for concentrated slurry flows ($\phi_v > 5\text{-}10\%$). Refractive index matching (RIM) is extensively used in the investigation of fluidized bed and slurry flows, flow through complex geometries and flow through porous media in conjunction with an optical diagnostic technique [10]. For example, RIM was used to investigate turbulent Taylor-Couette flow through the curved walls of two concentric cylinders [11]. A combination of RIM and PIV has also been used to optically measure the single-phase flow properties in porous structures [12]. Particle collisions in a liquid fluidized bed were investigated using RIM and PTV [13]. In recent years the use of RIM in concentrated particle suspension flows has allowed access for measurement by matching the refractive index of the carrier phase and dispersed phase removing the effects of light refraction at phase boundaries. RIM provides optical access for illumination and image acquisition for optical visualization for PIV. While the principle of refractive index matching is simplistic, in practice the experiments are sensitive to many parameters including control of liquid phase refractive index (through concentration and temperature of the solution used to produce RIM), impurities present in the particles or in the liquid phase, and temperature gradients within the suspension [10]. Early attempts were made to study turbulent slurry pipe flows using optical technique with RIM [1][14][15]. Refractive index facility in conjunction with LDV has been utilized to discriminate solid and liquid phase velocities in the slurry flowing in a horizontal pipe [1]. A combination of RIM and LDV was used to investigate liquid turbulence modification in the presence of 53 μm size particles in pipe flow for low ϕ_v ($< 6\%$) [14]. Particle mean and root mean square velocities were measured using LDV and RIM in solid-liquid turbulent flow in a vertical pipe containing 270 μm mean diameter sized spherical particles for $\phi_v < 14\%$ [15].

The present study discusses a PIV approach in conjunction with RIM to attain optical transparency. A description of a vertical slurry pipe loop experimental facility used initially to make PIV measurements with dilute two-phase flows is described, and some of those results, obtained through particle masking processing techniques, are presented. Liquid phase turbulent statistics for a dilute solid-liquid flow ($\phi_v < 1\%$) are described. Finally, a novel refractive index matched solution, aqueous potassium thiocyanate solution (KSCN), is also investigated.

2 Experimental methodology

2.1 Set-up of the vertical flow loop

A schematic of the vertical slurry pipe loop experimental facility is shown in Fig. 1. Dilute two-phase experiments were initially carried out in a vertical flow loop. For the dilute slurry, water and nearly monosized glass beads (mean diameter 2 mm) were used as continuous and dispersed phases respectively. The slurry was pumped from a feed tank into the vertical loop in the upward direction by a centrifugal pump (2×1.5 WX-B, Battlemountain). The vertical loop was made of stainless steel, had an inner diameter $D = 50.6$ mm and was 6.5 m long in each of the upstream and downstream vertical sections. To measure the flow rate, a magnetic flow meter (IMT25, Foxboro) was located at the beginning of the upstream section of the loop. A variable frequency drive (Altivar 61, Schneider Electric) connected to the slurry pump was used to maintain the desired flow rate. A double pipe heat exchanger was installed in the upstream section of the loop to maintain temperature of the mixture. All experiments were conducted under isothermal conditions at a mixture temperature of 25°C. Experiments were conducted in the closed (recirculating) mode by isolating the vertical loop from the feed tank.

The test section was made of transparent acrylic to allow optical access and measurements were carried out at the location 90D above the bottom position of the loop to ensure fully developed flow. The circular test section of the vertical loop was surrounded by a square viewing box made of transparent acrylic and filled with water to minimize image distortion due to the circular curvature of the test section wall during PIV measurements. At the start of the experiments, particles were introduced manually into the feed tank. Before starting the PIV measurements, purging of entrained air was necessary to avoid the presence of air bubbles in the flow.

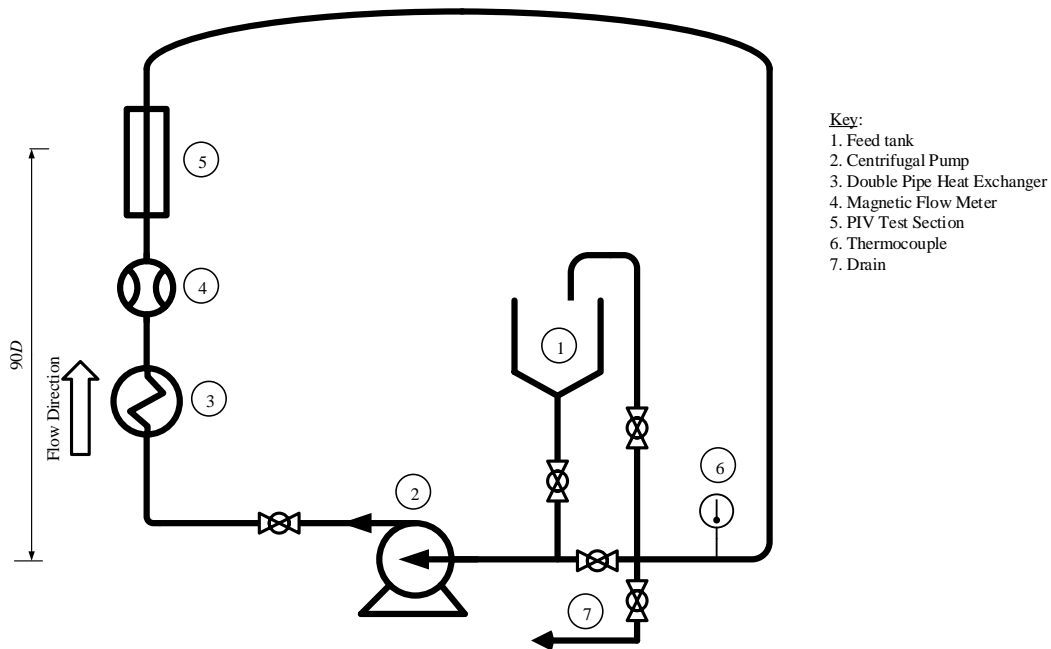


Fig. 1: Schematic diagram of vertical pipe flow loop

2.2 PIV configuration

The PIV measurements were undertaken using the measurement set-up shown in the schematic in Fig. 2. Study of the liquid-phase velocity and turbulence in solid-liquid two phase flows in the pipe test section were made possible using measurements obtained with a commercial PIV system (LaVision GmbH.). The optical system was able to measure two-dimensional flow field. The liquid-phase was seeded with 18 μm tracer particles that followed motion of the turbulent flow. A 50 mJ double pulse Nd:YAG laser @ 532 nm (Solo III-15z, New Wave) illuminated the flow which was imaged using a 1376 \times 1040 pixels CCD camera (Imager Intense, LaVision GmbH.). A combination of cylindrical lenses and spherical telescope attached to the laser set-up was used to create a thin laser sheet. The time interval between two laser pulses and two frames was optimized based on the flow conditions and all timing signals were controlled and synchronized using a central pulse generator.

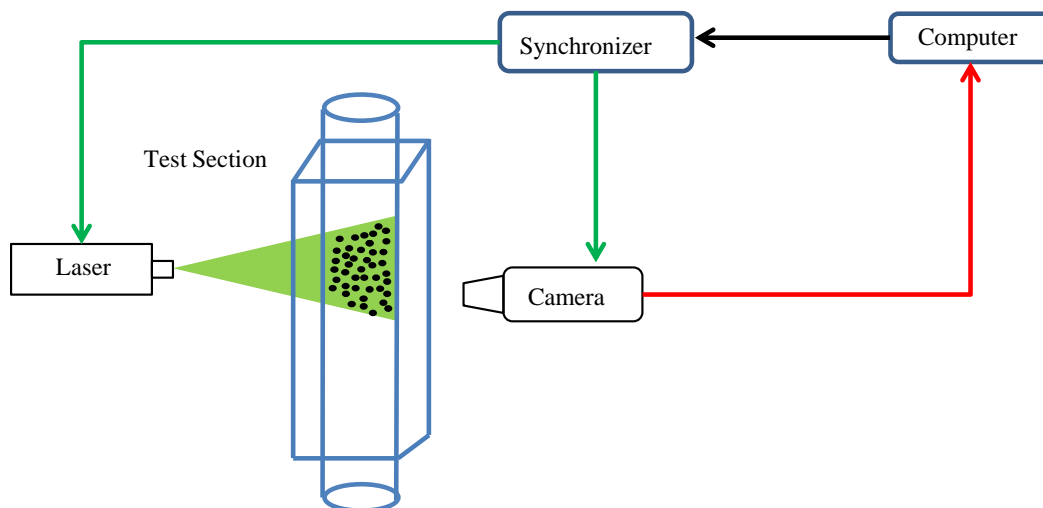


Fig. 2: Optical PIV measurement system

3 PIV processing with particle masking for particle concentration $\phi_v=0.8\%$

The PIV set-up was utilized to obtain 10,000 pairs of double frame raw images. An example of a sample raw PIV image containing both tracer particles (carrier phase) and glass beads (dispersed phase) is shown in Fig. 3(a) where $r/R = 0$, $r/R = 1$, and x/R represent pipe centreline, pipe wall and axial upward direction, respectively, normalized with pipe radius, R . A commercial algorithm (imfindcircle.m: MATLAB-R2013a, The Mathworks Inc.) was used to detect the glass beads. This function is based on a Hough transform for detection of circular objects. Two input parameters, a gradient-based threshold for edge detection and acceptable slurry particle radius range were required for the algorithm. Particle radius range was set to $\pm 20\%$ of average particle radius to detect all in-focus and out-of-focus particles. A low threshold was applied to detect particles from both frames of the raw images for PIV analysis of liquid phase. The detected dispersed phase particles in the images as shown in Fig. 3(b) were masked out for processing to calculate the liquid phase velocity field.

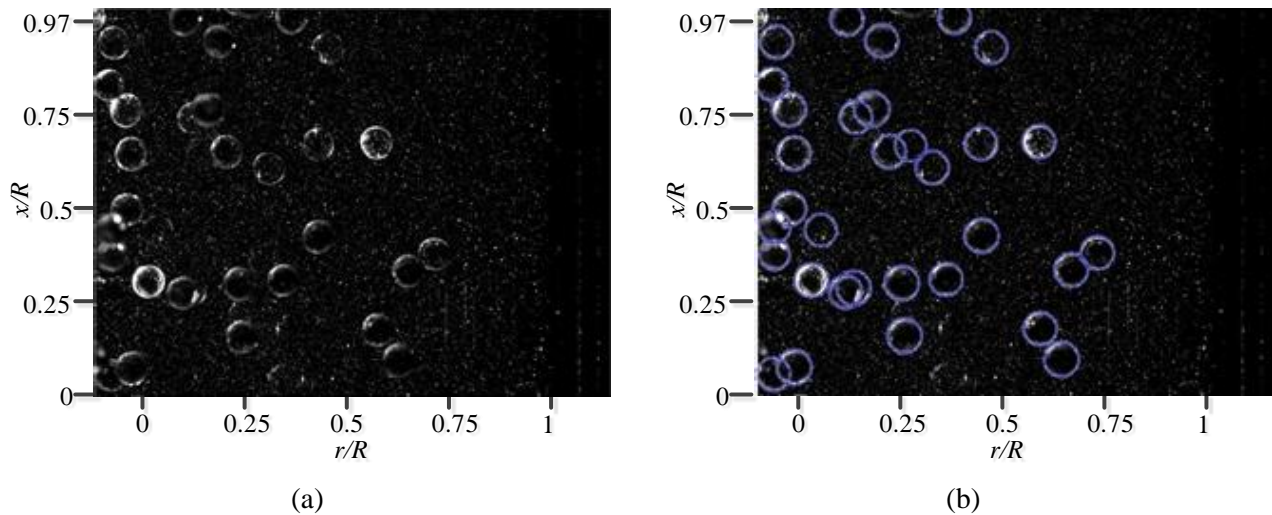


Fig. 3: PIV images for $\phi_v=0.8\%$, 2 mm glass beads: (a) Raw image (b) Detected glass beads

Additionally, two non-linear filters were applied for background correction and particle image normalization to increase the signal-to-noise (S/N) ratio. Finally, cross-correlation of double frame images with 32×32 pixel window size and 75% window lap was used to obtain instantaneous liquid phase velocities. Mean and fluctuating velocity components were obtained in both axial and radial direction by averaging all 10,000 pairs of images.

4 Turbulent fluctuation velocity profiles for dilute slurry flow

Variation in turbulent fluctuation velocity profiles at Reynolds number $Re=320,000$ in the presence of monosized 2 mm particles are presented for $\phi_v=0.8\%$. Axial turbulent fluctuation liquid velocity profile in the radial direction for single-phase (water only) and two-phase (water with glass beads) is shown in Fig. 4(a) where r and R are radial distance and pipe radius respectively. Axial turbulent fluctuation of liquid phase $\langle u'^2 \rangle$ does not have any significant effect due to addition for 2 mm size particles. However, small augmentation in fluid turbulence is observed near the wall as shown in Fig. 4(a) where $r/R=0$ and $r/R=1$ represent pipe centreline and pipe wall location respectively. Fig. 4(b) shows the liquid phase radial fluctuating velocity profiles for the two-phase case and the single-phase (water only) case. A small deviation in the radial velocity fluctuation of the liquid phase $\langle v'^2 \rangle$ is noticed in the presence of beads in comparison to the single-phase flow. 2 mm size particles introduce augmentation in the radial turbulent intensity in two-phase over single-phase flow. However, the axial and radial turbulence modulation i.e. the extent of change in fluid turbulence in the presence of particles is found to be below 5% at any point. Therefore, there is no substantial change in axial and radial

turbulent fluctuating velocity profile for liquid phase in dilute slurry flow. This slurry concentration is on the very low side of what is used in industry and high concentration slurry flows experiments are needed to investigate turbulence modulation effects at high Reynolds numbers.

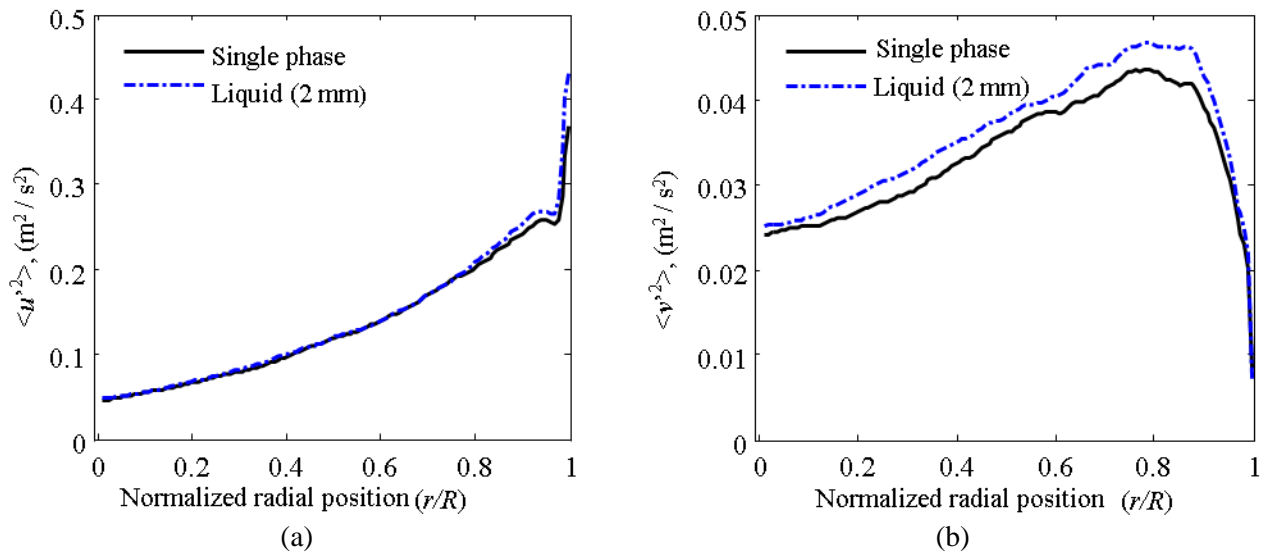


Fig. 4:(a) Axial (b) radial turbulent fluctuation velocity profiles of liquid phase

5 Refractive index matching

An aqueous solution of sodium iodide (NaI) with a borosilicate (Pyrex) solid is one of the more popular index-matched fluid/solid pairs and has been used in several applications for turbulence measurement in slurry flows [16]. However, an NaI solution only remains colorless and transparent for a couple of hours after its preparation with exposure to oxygen [16]. The NaI salt is expensive and relatively toxic making it difficult to use for large scale studies. An alternative index-matched fluid is aqueous potassium thiocyanate (KSCN), which is less expensive and less toxic compared to aqueous NaI [17]. A KSCN solution also remains colorless and transparent indefinitely allowing the solution to be used for multiple studies over many years. There is no comprehensive study investigating the refractive index of KSCN in the literature. Despite the comparative paucity of information on its physical properties, KSCN solutions have been used as index-matched fluids in several applications, e.g. [13].

To define the optical properties of a KSCN solution, its refractive index was measured up to its solubility limit at a wavelength of 589 nm using a refractometer (Abbe-3L, Bausch and Lomb) at different temperatures (T). During the tests, the mass concentration of the KSCN in demineralized water solutions was varied. The concentration (c) is defined as the ratio of KSCN mass to the total mass of the solution. The preparation of KSCN solutions requires heat input as the salt dissolution is an endothermic reaction. At room temperature (23 °C), the solubility of KSCN was estimated based on the maximum mass of salt that can be dissolved while avoiding crystal formation. Saturated KSCN solution ($c = 70.5\%$) was prepared and its concentration was varied from 70.5-20% by adding a measured amount of water using a syringe and stirring the solution until well mixed. Refractometer measurements were made at different salt concentrations and a constant temperature. The temperature of the KSCN solution was maintained at a constant temperature in the 25-40 °C range using a programmable temperature controller (Polystat, Cole-Parmer) connected to the refractometer.

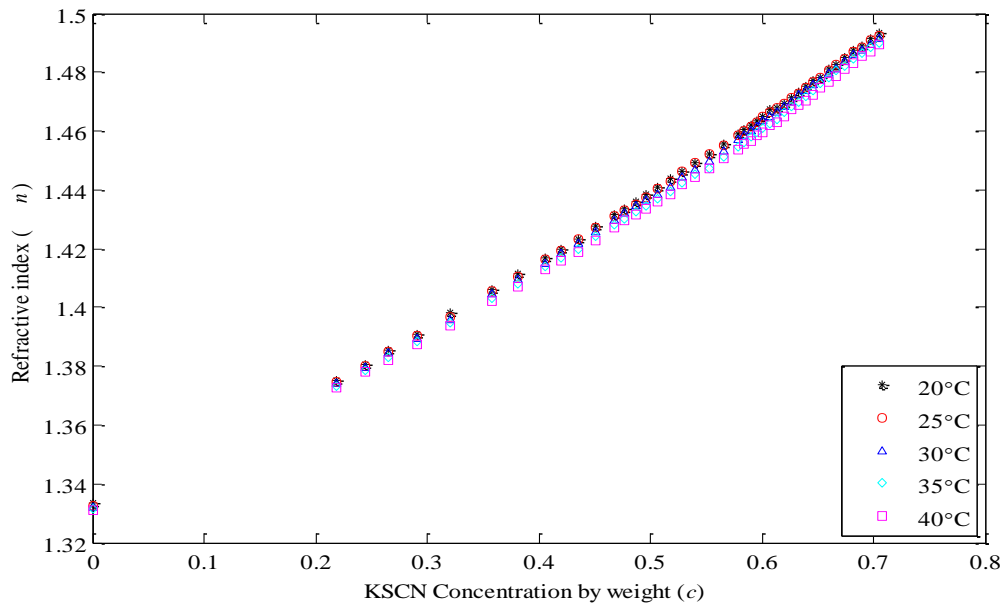


Fig. 5: Refractive index of a KSCN solution as a function of salt concentration and solution temperature

Refractive index measurements were made at temperatures $T = 20, 25, 30, 35, 40$ °C and the results are shown in Fig. 5. The refractive index was controlled from the base value of pure water, $n = 1.3308$ to a maximum of $n = 1.4931$ for a KSCN concentration of $c = 70.5\%$ at a constant temperature in the 25-40°C range. The refractive index of KSCN increases continuously with concentration in the same nonlinear manner for all salt solution temperatures as shown in Fig. 5. There is no significant decrease in refractive index with increasing temperature for the concentration and temperature ranges tested here.

The solution refractive index is known to be sensitive to temperature and concentration changes which can make it difficult to index-match the fluid with the dispersed phase. The present work and the literature [16] on the refractive indices of KSCN and NaI solutions suggest that the temperature sensitivity for both solutions is quite similar. The concentration sensitivity for both salt solutions was investigated at $T = 25$ °C. The concentration range $c = 54-66\%$ was chosen for sensitivity analysis of both the fluids as it overlaps with the refractive index of borosilicate glass which has a documented value of $n = 1.473$ (Leon Parson, Chemglass Life Sciences, personal communication Oct 2014). The results are plotted in Fig. 6: a linear, least-squares fit to all data for aqueous NaI and KSCN gives:

$$n_{\text{NaI}} = 0.3982 c + 1.2427 \quad \rightarrow \quad \frac{dn_{\text{NaI}}}{dc} = 0.3982 \quad (1)$$

$$n_{\text{KSCN}} = 0.2605 c + 1.3082 \quad \rightarrow \quad \frac{dn_{\text{KSCN}}}{dc} = 0.2605 \quad (2)$$

The data fits well with the empirical correlation having $R^2 = 0.9994$ and 0.9992 for KSCN and NaI respectively. Equations (1) and (2) show that the refractive index gradient for NaI and KSCN with concentration is 0.3982 and 0.2605, respectively; in other words, the gradient for the NaI solution is 1.53 times greater than that of the KSCN solution. This indicates that the refractive index of KSCN is much less sensitive with concentration changes than NaI, highlighting that as an index matched fluid for RIM, it will be easier to establish and maintain index matching within an experiment.

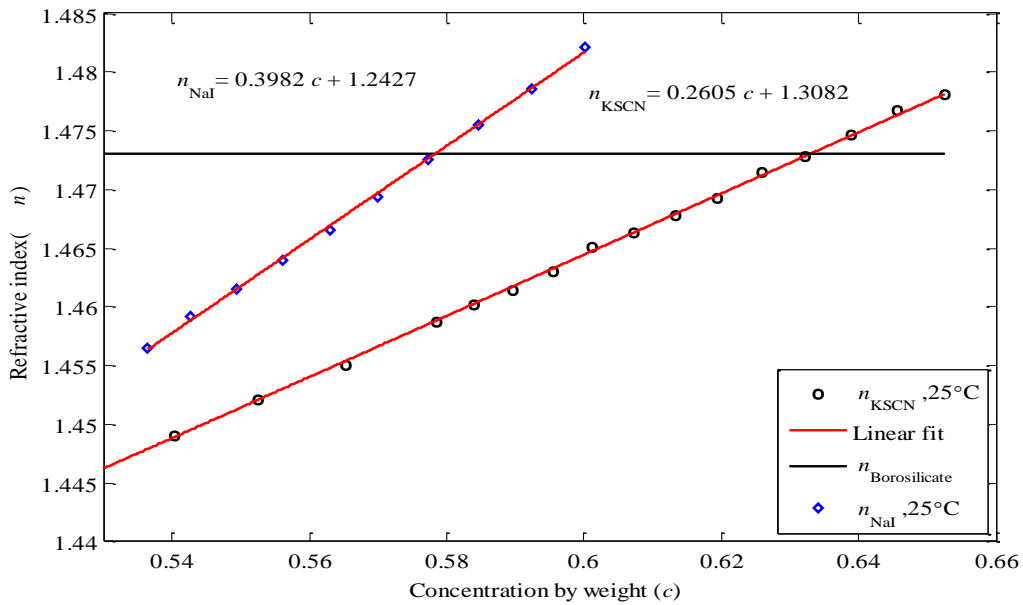


Fig. 6: Gradient of KSCN and NaI solution for concentration sensitivity

The refractometer measurements provide quantitative analysis of the refractive index of KSCN but do not consider any optical analysis for index matching with a borosilicate bead typically used as the dispersed phase in experiments. For this purpose, a rectangular beaker 6.5 cm in depth was filled approximately half with diameter 3 mm size beads in a packed bed. In addition, a calibration target was placed on the mid-plane of the beaker as an image reference. There were at least 22 interfaces of solids-fluid to cross to see through to the calibration target. Each interface creates slight mismatch in refractive index causing image deformation. Fig. 7 shows an image of the calibration target taken with a 2048×2048 pixels camera (TM-4200GE, JAI) as KSCN concentration is changed in the beaker. For the perfect RIM, solid particles should be invisible and background target behind them should be undistorted [16]. Fig. 7 displays images of the calibration target with its visible calibration dots in the packed bed for $c = 68.2$, 62.4 and 60.8% respectively. At $c = 68.2\%$ (Fig. 7a), the bottom half of the target is not visible because light is dispersed due to the presence of beads. Decreasing the KSCN concentration draws the refractive index of the liquid and solid together allowing undistorted images of the target dots to appear. Target dots are completely visible at $c = 62.4\%$ where no light is refracted by the beads. Nevertheless, further decreasing the concentration develops a mismatch in refractive index and there is an observed distortion in the images of the target dots as shown for $c = 60.8\%$ in Fig. 7(c).

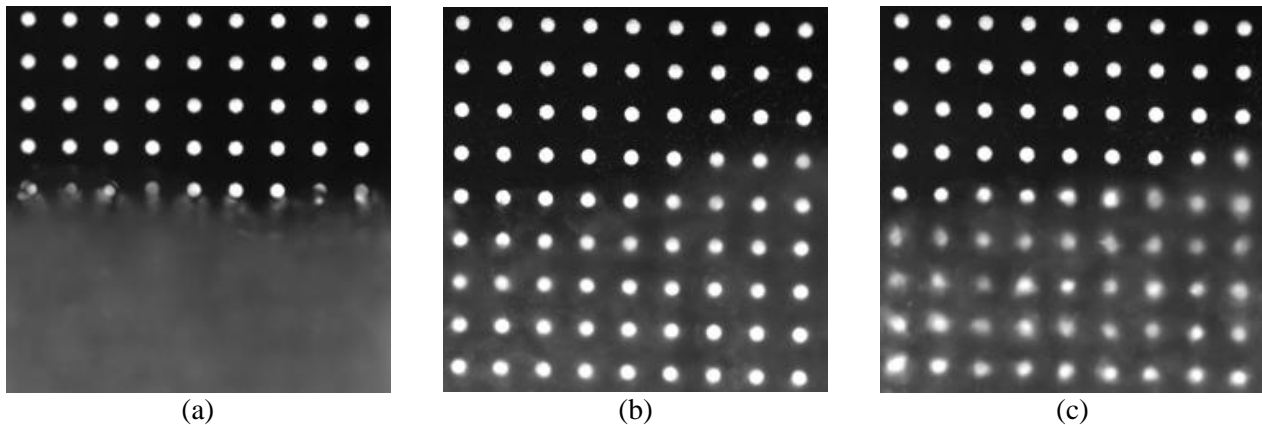


Fig. 7: Calibration target in packed bed beads for KSCN concentration (a) 68.2 (b) 62.4 (c) 60.8% w/w

Measurements of the density using a pycnometer and dynamic viscosity using a rheometer (AR-G2, TA Instruments) of KSCN of $c = 62.4\%$ are tabulated in Table 1. The KSCN solution is Newtonian and has a dynamic viscosity 2.3 times greater than water. Its density was found to be $1,310 \text{ kg/m}^3$. Generally, the KSCN solution properties make it a reasonable fluid analog for the study of turbulence in slurry flows.

Table 1: Properties of index matched KSCN solution at 25°C

Density (ρ)	1310 kg/m ³
Dynamic viscosity(μ)	2.2 mPa-s

6 Conclusions

A vertical pipe loop ($D = 50.6 \text{ mm}$) has been used for a slurry flow study. Water and glass beads are used as carrier and dispersed phase, respectively. Instantaneous liquid phase velocities were obtained by PIV processing in combination with particle masking. Axial and radial fluctuating velocities (for the liquid phase) in the presence of 2 mm glass bead in water for $\phi_v = 0.8\%$ at $Re = 320,000$ are reported. There appears to be no significant effect on the fluid turbulence for these particular particles at this low concentration and high flow Reynolds number. Additionally, the ability to using refractive index matching to eliminate strong refraction from phase boundaries and create optical transparency has been explored. An alternative index matching fluid (aqueous KSCN solution) is characterized. A wide range of refractive index values ($n = 1.3308 - 1.4931$) for different mass concentrations of KSCN ($c = 70.5\%$) was obtained for temperatures from 20 to 40°C. Refractive indices of KSCN solutions were observed to increase continuously with concentration in a nonlinear fashion for all salt solution temperatures. There was no substantial decrease in the refractive index with increasing temperature for the tested concentration and temperature ranges. Refractive index gradient with concentration of a conventional RIM salt, NaI, is 1.53 times greater than was measured for a KSCN solution. This indicates that KSCN is less concentration sensitive and potentially more stable in experiments. Calibration images show that the optical transparency of the index-matched mixtures is excellent for close-packed beads using 3 mm diameter borosilicates beads and $c = 62.4\%$ KSCN concentration.

Acknowledgements

The authors gratefully acknowledge financial support from Natural Sciences and Engineering Research Council (NSERC) of Canada the Alberta Ingenuity Fund, the Canadian Foundation for Innovation (CFI), and the NSERC Industrial Research Chair in Pipeline Transport Processes (RSS).

References

- [1] Chen R C, Kadambi J R (1995) Discrimination between solid and liquid velocities in slurry flow using laser Doppler velocimeter. *Journal of Powder Technology*, vol. 85, pp. 127–13.
- [2] Balachandar S, Eaton J K (2010) Turbulent dispersed multiphase flow. *Annual Review Fluid Mechanics*, vol. 42, pp. 111–133. doi:10.1146/annurev.fluid.010908.165243.
- [3] Crowe, C T (2000) On models for turbulence modulation in fluid-particle flows. *International Journal of Multiphase Flow*, vol. 26, pp. 719–727.
- [4] Hosokawa S, Tomiyama A (2004) Turbulence modification in gas–liquid and solid–liquid dispersed two-phase pipe flows. *International Journal of Heat and Fluid Flow*, vol. 25, pp. 489–498. doi: 10.1016/j.ijheatfluidflow.2004.02.001.
- [5] Kim S, Lee K B, Lee C G (2005) Theoretical approach on the turbulence intensity of the carrier fluid in dilute two-phase flows. *International Journal of Heat and Mass Transfer*, vol. 32, pp. 435–444. doi:10.1016/j.icheatmasstransfer.2004.07.003.

- [6] Budwig R (1994) Refractive index matching methods for liquid flow investigations. *Experiments in Fluids*, vol. 17, pp. 350–355. doi:10.1007/BF01874416.
- [7] Merzkirch W (1997) PIV in multiphase flow. In: Proceeding of the Second International Workshop on PIV-Fukui, pp. 165–171.
- [8] Brücker C (2000) PIV in two-phase flows. Lecture Series on Particle Image Velocimetry and Associate Technique. Jan. 17-21, pp. 1–28.
- [9] Cui M M, Adrian RJ (1997) Refractive index matching and marking methods for highly concentrated solid-liquid flows. *Experiments in Fluids*, vol. 22, pp. 261–264.
- [10] Wiederseiner S, Andreini N, Epely-Chauvin G, Ancey C (2010) Refractive-index and density matching in concentrated particle suspensions. A review article: *Experiments in Fluids*, vol. 50, pp. 1183–1206. doi:10.1007/s00348-010-0996-8.
- [11] Parker J, Merati P (1996) An investigation of turbulent Taylor-Couette flow using laser Doppler velocimetry in a refractive index matched facility. *Journal of Fluids Engineering*, vol. 118, pp. 810-818.
- [12] Häfeli R, Altheimer M, Butscher D, Rudolf von Rohr P (2014) PIV study of flow through porous structure using refractive index matching. *Experiments in Fluids*, vol. 55, pp. 1717-x.
- [13] Aguilar-Corona A, Zenit R, Masbernat O (2011) Collisions in a liquid fluidized bed. *International Journal of Multiphase Flow*, vol. 37, pp. 695–705.
- [14] Zisselmar R, Molerus, O (1979) Investigation of solid-liquid pipe flow with regard to turbulence modification. *Journal of Chemical Engineering*, vol. 18, pp. 233–239.
- [15] Nouri J M, Whitelaw J H, Yianneskis, M (1987) Particle motion and turbulence flows in dense two-phase flows. *International Journal of Multiphase Flow*, vol. 13, pp. 729–739.
- [16] Bai K, Katz J (2014) On the refractive index of sodium iodide solutions for index matching in PIV. *Experiments in Fluids*, vol. 55, pp.1704-x. doi:10.1007/s00348-014-1704-x.
- [17] Hassan Y A and Dominguez-Ontiveros E E (2008) Flow visualization in a pebble bed reactor experiment using PIV and refractive index matching techniques. *Journal of Nuclear Engineering and Design*, vol. 238, pp. 3080–3085.